Polarization of holographic grating diffraction. II. Experiment

Tsu-Wei Nee and Soe-Mie F. Nee

Research Department, Naval Air Warfare Center, China Lake, California 93555-6100

Mark W. Kleinschmit

Digital Optics Technologies, Rolling Meadows, Illinois 60008

M. S. Shahriar

Department of Electrical and Computer Engineering, Northwestern University, Evanston, Illinois 60208, and Research Laboratory of Electronics, Massachusetts Institute of Technology, Cambridge, Massachusetts 02139

Received July 16, 2003; revised manuscript received October 21, 2003; accepted November 20, 2003

The transmittance, ellipsometric parameters, and depolarization of transmission, diffraction, and reflection of two volume holographic gratings (VHGs) are measured at a wavelength of 632.8 nm. The measured data are in good agreement with the theoretical simulated results, which demonstrated the correlation between the diffraction strength and the polarization properties of a VHG. Vector electromagnetic theory and polarization characterization are necessary for complete interpretation of the diffraction property of a VHG. The diffraction efficiency is measured at 532 nm in a polarization-sensing experiment. The measured data and theoretical simulation have demonstrated the potential application of the holographic beam splitter for polarization-sensor technology. © 2004 Optical Society of America

OCIS codes: 050.1950, 090.1970, 090.7330, 260.5430, 260.1440.

1. INTRODUCTION

The holographic multibeam device is a holographic plate that works as a holographic laser beam combiner/splitter (HBCS). It is a device with multiple diffraction gratings. The full polarization property of diffraction by a volume holographic grating (VHG) was investigated theoretically in the preceding paper in this issue.[1] By using a simple volume grating model, we derived the diffracted fields and the Mueller matrices from Maxwell's equations, using Green's function algorithms. We investigated and formulated the polarization property of VHG diffraction with weak and strong coupling between the transmitted and the diffracted beams. We then derived and simulated the Mueller matrices of the diffraction and the transmitted beams by choosing appropriate parameters. In this paper we measure the polarization properties of two VHG samples and compare them with those predicted by the theory developed in Ref. 1. The measured optical properties of the quinine-doped polymethyl methacrylate (PMMA) substrate are reported in Section 2. The measured data of single- and three-hologram VHG samples (A and B), respectively, are reported in Section 3. Theoretical simulation results are presented in Section 4 and compared with the experimental data. An experiment demonstrating the polarization sensing of the three-hologram grating sample (B) and a theoretical justification are reported in Section 5. A discussion and conclusion are presented in Section 6.

2. OPTICAL PROPERTIES OF SUBSTRATE MATERIAL

The substrate material is made of phenanthraquinone-doped PMMA. As part of the holographic development procedure, the substrate was subjected to a ~60 °C bake for 12 h and then exposed to a mercury lamp (with its UV radiation blocked) for 2 h. The spectral index of refraction n and the extinction coefficient κ of the substrate were measured for wavelengths between 500 and 1600 nm. A halogen lamp and lasers at wavelengths 514, 544, and 633 nm were used as light sources for the measurements. n was determined by measuring the ellipsometer parameter ψ of reflection near the Brewster angle,[2,3] and κ was obtained by fitting the ratio of the measured transmittance at normal incidence to the transmittance calculated from the measured n. The measured n and κ are shown in Fig. 1. The κ curve is consistent with the previously reported absorption spectrum of PMMA.[4] Birefringence was observed in this substrate. The birefringence δn was obtained from the transmission retardation Δ measured at different incidence angles. Δ was determined by null ellipsometry. With a He–Ne laser source, δn was measured as 3.42×10^{-5} at a wavelength of 632.8 nm.

1084-7529/2004/040532-08$15.00

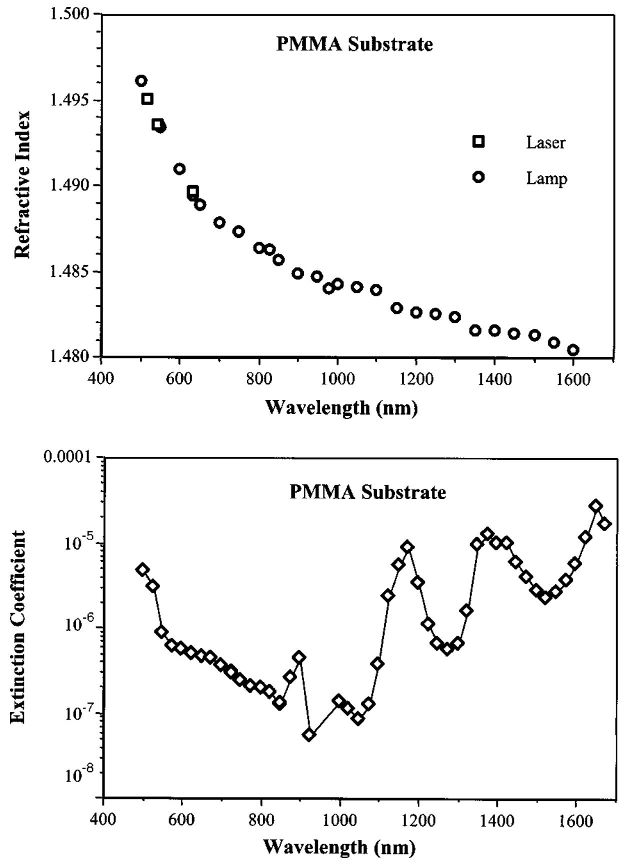

Fig. 1. Measured optical properties of the PMMA substrate material: top, refractive index; bottom, extinction coefficient in the spectral range 450–1700 nm.

3. OPTICAL PROPERTIES OF VOLUME HOLOGRAPHIC GRATINGS: EXPERIMENTS

A. Samples

Two uncoated VHG samples were investigated. Sample A is a 2-mm-thick uncoated holographic beam combiner (HBC) substrate containing a single VHG. Sample B is 1.71 mm thick and contains three VHGs. All hologram writings were performed on a floating optical table. The gratings were written in the substrate by using a frequency-doubled Nd–YVO_4 laser operating at 532 nm. Sample A was exposed for 90 s at a laser output power of 2.0 W, which was evenly divided into two Gaussian beams, each with a diameter of ~5 cm. For sample B, each grating was exposed for 70 s. The three gratings of sample B were designed to have the same incidence angles at a wavelength of 532 nm. However, the optical properties of both VHG samples were measured at a wavelength of 632.8 nm.

B. Diffraction Angles

The angles used in this paper are defined in Fig. 2. The z-axis is chosen along the normal of the sample plane. The x–z plane is chosen as the plane of incidence. θ_i, θ_t, and θ_r (all equal to θ) represent the angles of incidence, specular transmission, and reflection, respectively. $\Theta_t\,(=\Theta)$ and Θ_r represent, respectively, the polar angles of the transmissive diffraction and the reflective diffraction. Φ denotes the azimuthal angle of the diffraction beams. The direction of grating vector $\mathbf{K}\,(\theta_K,\ \phi_K)$ is perpendicular to the planes of the gratings. The three gratings of sample B were designed such that their corresponding $\mathbf{K}$ vectors fall on the same plane ($\phi_K = 0°$). Each sample was aligned such that $\mathbf{K}$ is also in the plane of incidence. The diffracted beams of both sample A and sample B are all in the plane of incidence so that $\Phi = 180°$ for all measurements. Sample A has maximum diffraction at $\theta = 29.55°$, $\Theta = 15.97°$. From these data, $\theta_K = 4.3444°$ and the grating spacing $x_0 = 821.3\,\text{nm}$ are determined by the photon-momentum relation [Eqs. (15) and (24b) of Ref. 1]. The results for both samples are listed in the top part of Table 1. Note that the incidence angles for the three gratings of sample B are different at a wavelength of 632.8 nm. The diffraction angles of sample B that have the same incidence angle $\theta = 2.17°$ at a wavelength of 532 nm are listed in the bottom part of Table 1.

C. Polarization

The principal Mueller matrix for reflected, transmitted, or deflected beam in the plane of incidence can be expressed as[5–7]

$$\mathbf{M} = R\begin{bmatrix} 1 & \mathcal{P}_x & 0 & 0 \\ \mathcal{P}_x & 1 - 2\mathcal{D}_v & 0 & 0 \\ 0 & 0 & \mathcal{P}_y & \mathcal{P}_z \\ 0 & 0 & -\mathcal{P}_z & \mathcal{P}_y \end{bmatrix}, \tag{1}$$

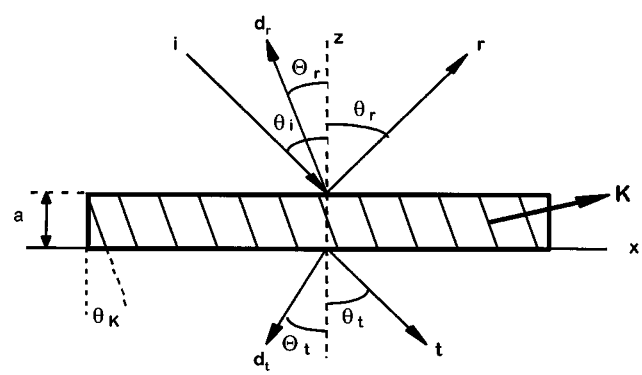

Fig. 2. Reflected, transmitted, and diffracted beams of the holographic grating sample.

Table 1. Volume Gratings' Diffraction Properties

Sample Grating	A	B1	B2	B3
Sample A[a]				
θ (deg)	29.55	4.77	5.32	5.85
Θ (deg)	15.97	27.80	34.32	40.91
θ_K (deg)	4.3444	−7.52	−9.33	−11.08
x_0 (nm)	821.25	1141.6	951.09	820.58
Sample B[b]				
θ (deg)		2.17	2.17	2.17
Θ (deg)		25.10	30.93	36.75

[a] $\lambda = 632.8\,\text{nm}$, $n = 1.4899$, $m = -1$, $\Phi = 180°$, $\phi_K = 0°$.
[b] $\lambda = 532\,\text{nm}$, $n = 1.4942$, $m = -1$, $\Phi = 180°$.

Table 2. Polarization Properties of Sample A at Wavelength 632.8 nm[a]

	Transmission (T_t)		Diffraction (T_d)		Reflection (R_r)
	Measured	Calculated	Measured	Calculated	(Measured)
R	0.703	0.864	0.226	0.055	0.071
ψ	48.08	46.50°	36.95°	36.95°	34.84°
Δ	29.21	29.20°	35.04°	35.01°	173.92°
$\mathcal{D}$	0.015	0.000	0.128	0.000	0.033
$\mathcal{D}_v$	0.007	0.000	0.002	0.000	0.002
$\eta = T_d/(T_t + T_d)$			0.243	0.059	

[a] Calculation parameters: $n = 1.4899$, $A_{\mathrm{pol}} = 1.183 \times 10^{-4}$, $Cdn = -4.4$, $\Delta\delta_a = 4.10°$, $\Delta\delta_b = 33.22°$, $dn/n = -3.49 \times 10^{-4}$.

where R is either transmittance or reflectance and $\mathcal{P}_x$, $\mathcal{P}_y$, and $\mathcal{P}_z$ are, respectively, the linear, preserved, and circular polarizations. Polarization $\mathcal{P}$ and depolarization $\mathcal{D}$ are defined by

$$\mathcal{P} = (\mathcal{P}_x{}^2 + \mathcal{P}_y{}^2 + \mathcal{P}_z{}^2)^{1/2}, \tag{2}$$

$$\mathcal{D} = 1 - \mathcal{P} = \mathcal{D}_u + \mathcal{D}_v, \tag{3}$$

where $\mathcal{D}_u$ and $\mathcal{D}_v$ are, respectively, the co- and cross-polarized parts of depolarization. $\mathcal{P}_x$, $\mathcal{P}_y$, and $\mathcal{P}_z$ are related to the ellipsometric parameters ψ and Δ by

$$\mathcal{P}_x = -\mathcal{P}\cos 2\psi, \tag{4a}$$

$$\mathcal{P}_y = \mathcal{P}\sin 2\psi \cos\Delta, \tag{4b}$$

$$\mathcal{P}_z = \mathcal{P}\sin 2\psi \sin\Delta, \tag{4c}$$

where ψ, Δ, $\mathcal{D}$, and $\mathcal{D}_v$ are four independent parameters in addition to R. They were measured with null ellipsometry.[6,7] The precise values of ψ and Δ for our null ellipsometers are 0.01° and 0.02°, respectively. The precise values of $\mathcal{D}$ and $\mathcal{D}_v$ are both 0.001. $\mathcal{P}$, $\mathcal{P}_x$, $\mathcal{P}_y$, and $\mathcal{P}_z$ were calculated by using Eqs. (2) and (4).

The measured and simulated properties for sample A are listed in Table 2. The properties of the reflective diffraction $R_d\,(m = -1)$ were not measured because of the limitation of the instrument. Nevertheless, R_d is small. The transmittances for specular transmission $T_t\,(m = 0)$ and transmissive diffraction $T_d\,(m = -1)$ are measured. The transmission diffraction efficiency $\eta = T_d/(T_t + T_d)$ were calculated and are shown in the last row of this table.

ψ and Δ are two independent parameters representing pure polarization. In Table 2 the ψ of diffraction is different from those of specular transmission and reflection. In general, $\psi > 45°$ for specular transmission and $\psi < 45°$ for specular reflection, which agreed with the measurements. It is interesting to see that $\psi < 45°$ for transmissive diffraction, in contrast to the specular transmission. Because the substrate is birefringent, the effect of the gratings on the measured retardation Δ is mixed with the retardation of the substrate. If the detected light contains only one kind of polarization, such as that of specular transmission or of pure direct diffraction, depolarization should be zero. If the detected light also includes other kinds of light, such as incoherent multiple reflection, depolarization will be appreciable. The not-small measured nonvanishing depolarization (0.128) of the diffracted beam indicates that the detected diffraction is not purely a direct diffraction. We may ignore the measured cross depolarization, because $\mathcal{D}_v$ is easily subject to the misalignment of the system with respect to the sample.

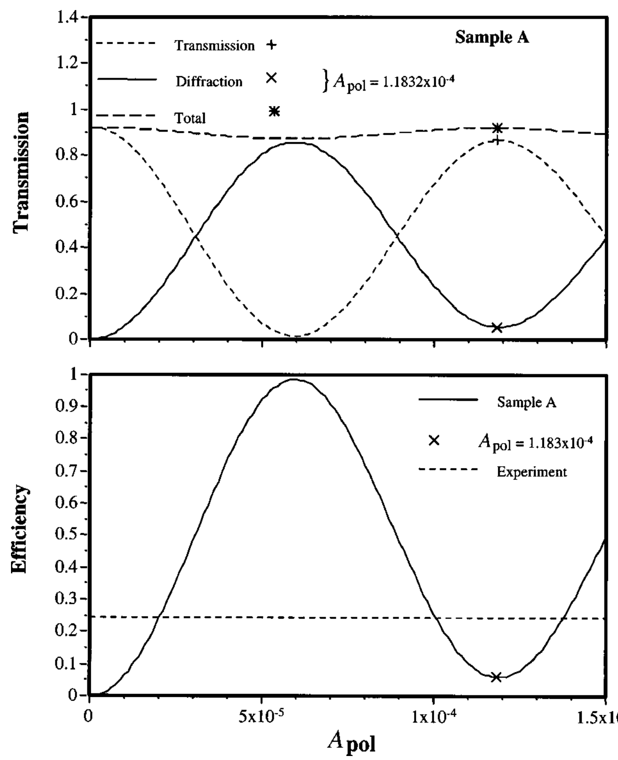

Fig. 3. Calculated transmittance of transmitted and diffracted beams (T_t and T_d) and transmission diffraction efficiency η for sample A. The parameters are listed in Table 2. The fitted points are marked by x.

4. OPTICAL PROPERTIES OF VOLUME HOLOGRAPHIC GRATINGS: THEORETICAL INTERPRETATION

For sample A, the theoretically simulated results of transmission T_a, diffraction T_b, and η are calculated for $A_{\mathrm{pol}} = 0$ to 1.5×10^{-4} and shown in Fig. 3.

$$A_{\mathrm{pol}} = \alpha/(A_u x_0) \tag{5}$$

is a dimensionless diffraction-strength parameter.[1] A_u is a constant with the dimension of area, and α (unit of volume) is the effective electric polarizability of the holographic grating at wavelength λ. The ellipsometric parameters ψ and Δ are shown in Fig. 4. For a numerical-model calculation, we use the Gaussian form of the normalized one-dimensional grating profile function $f(u)$:

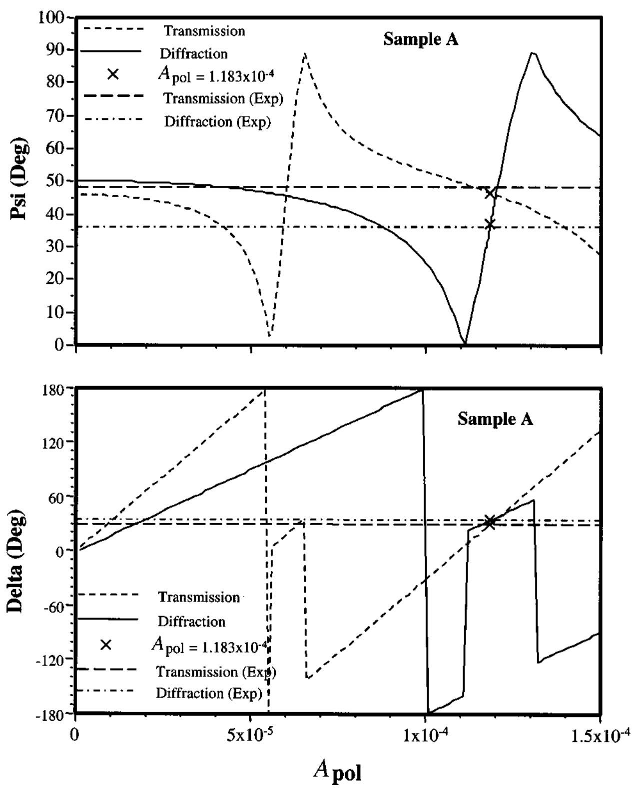

Fig. 4. Calculated ψ and Δ of sample A. Horizontal lines are the measured data; the fitted points are marked by x. Parameters are the same as in Fig. 3.

$$f(u) = \frac{1}{u_0\sqrt{\pi}}\exp\left(-\frac{u^2}{u_0{}^2}\right). \tag{6}$$

Since the holographic grating is fabricated by laser interference,[8,9] as shown in Fig. 5 of Ref. 1, $u_0 = 0.2821\,\mu$m is an acceptable choice (Fig. 5 of Ref. 1). The diffraction-strength parameter A_{pol} is determined by the measured data. As shown in Fig. 3, $A_{pol}(\eta)$ is not a unique-valued function of η. It is not appropriate to use only the measured η for determining the value of A_{pol}. Since the ellipsometrically measured ψ has higher accuracy than other parameters,[5–7] we would use $\psi(A_{pol})$ to determine the fitted parameter A_{pol}. In Fig. 4, the measured ψ shown in Table 2 are plotted as the horizontal lines. The solid and dashed curves are the diffracted and transmitted beams, respectively. $A_{pol} = 1.1832 \times 10^{-4}$ is a best-fit value fitting the ψ data of both the diffracted and the transmitted beams. The fitted ψ of the transmitted and diffracted beams are marked as "x." The corresponding T_t, T_d, and η are calculated from this fitted A_{pol}. They are shown as the marked points in Fig. 3. The measured intensity for the diffracted beam may also contain multiple reflected lights because the measured depolarization is large. Therefore the measured η $(=0.243)$ is considerable larger than the calculated value $(=0.059)$ when the ψ-fitted A_{pol} is used.

The one-dimensional volume grating would create additional birefringence, even though the substrate material does not have birefringence. Therefore there is an appreciable effect on the ellipsometric parameter Δ. To fit the measured data of Δ, we use an empirical birefringence model in which the average index of refraction of the beam with (Θ_j, Φ_j)-polarization-vector direction for the s or p wave is

Table 3. Mueller Matrix Properties at Wavelength 632.8 nm for Sample B

	Transmission (T_t)		Diffraction (T_d)		η	
	Measured	Calculated	Measured	Calculated	Measured	Calculated
Grating #1[a]						
$R(T_t, T_d)$	0.8661	0.9089	0.0199	0.0163	2.22×10^{-2}	1.76×10^{-2}
ψ	45.04°	45.03°	44.98°	44.97°		
Δ	−7.54	−7.56	5.541	5.56°		
$\mathcal{D}$	3.27×10^{-5}	0.000	3.29×10^{-3}	0.000		
$\Delta\delta$ (deg)		−49.81		33.18		
Grating #2[b]						
$R(T_t, T_d)$	0.8666	0.8905	0.0114	0.0373	1.30×10^{-2}	4.02×10^{-2}
ψ	45.05°	45.11°	43.56°	43.56°		
Δ	−7.34°	−7.32°	12.77°	12.82°		
$\mathcal{D}$	2.99×10^{-5}	0.000	8.15×10^{-3}	0.000		
$\Delta\delta$		33.85°		37.11°		
Grating #3[c]						
$R(T_t, T_d)$	0.8653	0.8588	0.0071	0.0765	8.16×10^{-3}	8.178×10^{-2}
ψ	45.04°	45.09°	45.34°	45.34°		
Δ	−7.27°	−7.29°	20.08°	20.02°		
$\mathcal{D}$	3.88×10^{-5}	0.000	2.22×10^{-2}	0.000		
$\Delta\delta$		−5.75°		40.10°		

[a] $(\theta, \Theta, \Phi) = (4.77°, 27.80°, 180°)$, $Cdn = -4.4$, $A_{pol} = 8.007 \times 10^{-5}$, $n = 1.4899$, $\mathcal{D}_v = \mathcal{D} = 0$, $dn/n = -2.36 \times 10^{-4}$.
[b] $(\theta, \Theta, \Phi) = (5.32°, 34.32°, 180°)$, $Cdn = -4.4$, $A_{pol} = 1.0411 \times 10^{-4}$, $n = 1.4899$, $\mathcal{D}_v = \mathcal{D} = 0$, $dn/n = -3.07 \times 10^{-4}$.
[c] $(\theta, \Theta, \Phi) = (5.85°, 40.91°, 180°)$, $Cdn = -4.4$, $A_{pol} = 1.402 \times 10^{-4}$, $n = 1.4899$, $\mathcal{D}_v = \mathcal{D} = 0$, $dn/n = -4.14 \times 10^{-4}$.

Table 4. Calculated Mueller Matrix Properties of Sample B, Grating #1, and Fitted Incident Stokes Vector (1, 0, U, 0) for Wavelength 532 nm, n = 1.4942[a]

	R	ψ (deg)	$M_{11}^{(j)}$	$M_{12}^{(j)}$	$M_{13}^{(j)}$	$M_{14}^{(j)}$
Experiment A[b]						
Transmission (t)	0.8126	45.67	0.8126	0.0190	0.0000	0.0000
Diffraction (d)	0.0398	42.10	0.0398	−0.0040	0.0000	0.0000
Experiment B[c]						
Transmission (t)	0.7683	39.56	0.7683	−0.1445	0.0000	0.0000
Diffraction (d)	0.0376	73.00	0.0376	0.0312	0.0000	0.0000
Experiment C[d]						
Transmission (t)	0.7854	49.37	0.7856	0.1193	0.0000	0.0000
Diffraction (d)	0.0385	11.40	0.0385	−0.0355	0.0000	0.0000

[a] $(\theta, \Theta, \Phi) = (2.17°, 25.10°, 180°)$, $(\theta_K, \phi_K) = (-7.52°, 0°)$, $x_0 = 1141.6$ nm

[b] $A_{\rm pol} = 4.327 \times 10^{-6}$, $Cdn = -4.4$, $\mathcal{D} = \mathcal{D}_v = 0$, $U = 0.22$.

[c] $A_{\rm pol} = 3.433 \times 10^{-5}$, $Cdn = -4.4$, $\mathcal{D} = \mathcal{D}_v = 0$, $U = -0.027$.

[d] $A_{\rm pol} = 4.167 \times 10^{-5}$, $Cdn = -4.4$, $\mathcal{D} = \mathcal{D}_v = 0$, $U = 0.025$.

$$n(\Theta_j, \Phi_j) = n_+ n_- /(n_+^2 \sin^2 \delta_j + n_-^2 \cos^2 \delta_j)^{1/2},$$

$$j = ts, tp, ds, dp, \tag{7a}$$

$$\cos(\delta_j - \Delta\delta_j) = \sin\Theta_j \cos\theta_K \cos(\Phi_j - \phi_K) + \cos\Theta_j \sin\theta_K. \tag{7b}$$

$\delta_j - \Delta\delta_j$ is the angle between the grating vector **K** and the propagation direction of the diffraction beam (Θ_j, Φ_j); dn $(=n_+ - n_-)$ is assumed proportional to the grating diffraction-strength parameter $A_{\rm pol}$,

$$dn = Cdn(A_{\rm pol}), \tag{8}$$

where Cdn is the strength parameter of grating induced birefringence. For simplicity, we assume that $\Delta\delta_j$ $(j = ts, tp, ds, dp)$ are the same for s and p waves. The parameters Cdn, $\Delta\delta_a$, $\Delta\delta_b$ are determined by fitting the measured Δ values. For sample A, these parameters and the grating-induced birefringence dn/n are listed in Table 2. The calculated parameters R, ψ, Δ, $\mathcal{D}_v$, $\mathcal{D}$, and η are also listed in Table 2. Agreement with the experiment is good. In Fig. 4 the measured Δ shown in Table 2 are plotted as the horizontal lines. The solid and dashed curves are the diffracted and the transmitted beams, respectively. $A_{\rm pol} = 1.1832 \times 10^{-4}$ is also a best-fit value fitting the Δ data of both the diffracted and the transmitted beams.

Since the statistical property of the Mueller matrix[5–7] was not considered in the dynamical theory,[1] there is no depolarization in the calculated results, $\mathcal{D} = \mathcal{D}_v = 0$ (Table 2). We made similar fitting to the measured data of sample B at 632.8 nm. The results are listed in Table 3. For a wavelength of 532 nm, the incidence angles of the three gratings of sample B are the same. The incident beam at $\theta = 2.17°$ (Tables 1 and 4) is split into four beams: the transmitted beam and three diffracted beams of angles $\Theta = 25.10°$, 30.93°, and 36.75°. Assuming that the three gratings have approximately equal statistical weight, the three diffracted beams' transmittances versus $A_{\rm pol}$ are calculated. The results are shown in Fig. 5. Sample thickness 1.71 mm and $u_0 = 0.2821$ μm are used for the calculation.[1]

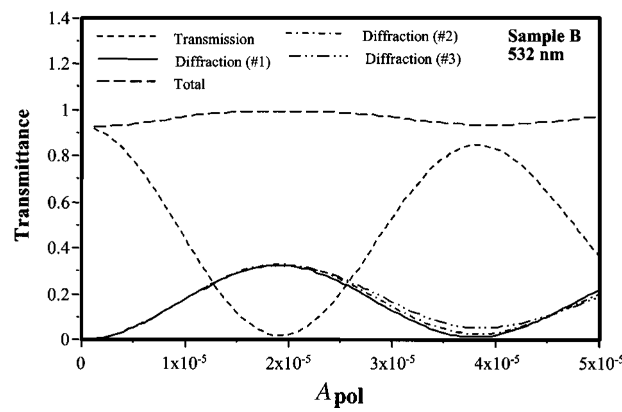

Fig. 5. Calculated transmittance of the transmitted and the three diffracted beams at wavelength 532 nm for sample B. Parameters are $n = 1.4942$, $u_0 = 0.2821$ μm, sample thickness = 1.71 mm. Other parameters are listed in Tables 1 and 4.

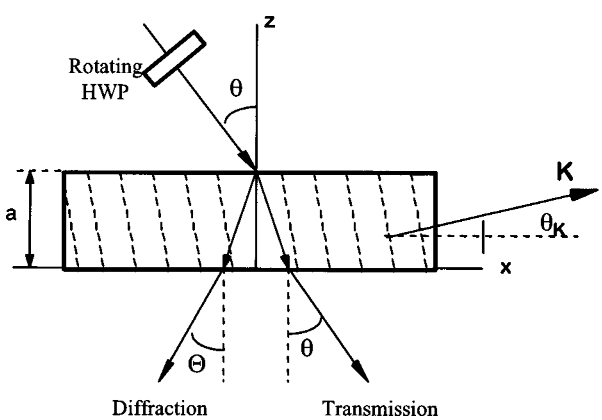

Fig. 6. Polarization-sensing experiment of sample B. HWP, half-wave plate.

5. POLARIZATION-SENSING EXPERIMENT

The polarization-filtering effect of the holographic beam splitter (HBS) is shown in the following experiment. As shown in Fig. 6, a rotating half-wave plate, HWP, is placed in the incident 532-nm laser path. Two identical detectors were used to measure the intensities of transmitted (t) and diffracted (d) beams. These measured dif-

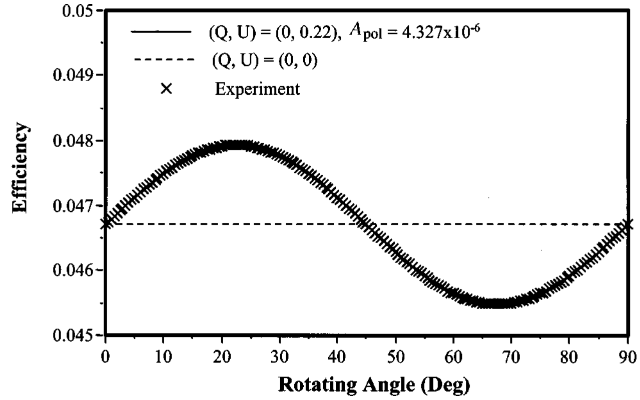

Fig. 7. HWP rotating angle (δ) dependence of the diffraction efficiency η at wavelength 532 nm. The measured data are marked by x. With $A_{\mathrm{pol}} = 4.327 \times 10^{-6}$, the solid curve is the calculated result with incident Stokes parameter (1, 0, 0.22, 0). Other parameters are listed in Table 4.

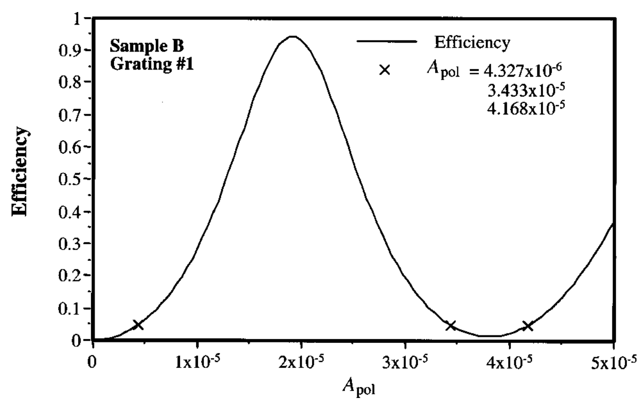

Fig. 8. Calculated diffraction efficiency η of grating #1 of sample B at wavelength 532 nm. Other parameters are listed in Table 4.

fraction signals are due to grating #1, $(\theta_K, \phi_K) = (-7.52°, 0°)$, $(\theta, \Theta, \Phi) = (2.17°, 25.10°, 180°)$. The Stokes vectors of the incident beam (i) and those of the transmission (t) and the diffracted (d) beams are related by the following relation,

$$\begin{pmatrix} I^{(j)} \\ Q^{(j)} \\ U^{(j)} \\ V^{(j)} \end{pmatrix} = \mathbf{M}^{(j)}\mathbf{M}_{\mathrm{hwp}}(\delta)\begin{pmatrix} I_i \\ Q_i \\ U_i \\ V_i \end{pmatrix}, \qquad j = t, d, \tag{9}$$

where

$$\mathbf{M}_{\mathrm{hwp}}(\delta) = T_{\mathrm{hwp}}\begin{bmatrix} 1 & 0 & 0 & 0 \\ 0 & \cos 4\delta & -\sin 4\delta & 0 \\ 0 & -\sin 4\delta & -\cos 4\delta & 0 \\ 0 & 0 & 0 & -1 \end{bmatrix} \tag{10}$$

is the Mueller matrix of the rotating half-wave plate of transmittance T_{hwp} and rotating angle δ (hwp stands for half-wave plate). The signals measured by the two sensor detectors (with the same detection constant s_d) are

$$S^{(j)}(\delta) = s_d I^{(j)}(\delta), \qquad j = t, d, \tag{11a}$$

$$\begin{aligned} I^{(j)}(\delta) = T_{\mathrm{hwp}}\{ & I_j M_{11}^{(j)} + (Q_j \cos 4\delta \\ & - U_j \sin 4\delta) M_{12}^{(j)} \\ & - (Q_j \sin 4\delta + U_j \cos 4\delta) M_{13}^{(j)} \\ & - V_j M_{14}^{(j)}\}, \\ & \qquad j = t, d. \end{aligned} \tag{11b}$$

$M_{1k}^{(j)}$ $(k = 1, 2, 3, 4)$ are the first-row Mueller matrix elements of the two beams t and d $[\mathbf{M}^{(j)}]$. The diffraction efficiency is

$$\eta(\delta) = I^{(d)}/(I^{(t)} + I^{(d)}) = S^{(d)}/(S^{(t)} + S^{(d)}). \tag{12}$$

For grating #1, the diffraction efficiency η versus δ is measured and shown in Fig. 7 (points marked x). The average value $\langle \eta \rangle = 0.0467$. With the parameters shown in Table 1, $\eta(A_{\mathrm{pol}})$ is calculated and shown in Fig. 8. There are three values of A_{pol}: (A) 4.327×10^{-6}, (B) 3.433×10^{-5}, and (C) 4.167×10^{-5}, with $\eta = 0.0467$. They are marked (x) in Fig. 8. For these three A_{pol}'s, the Mueller matrix properties are calculated and shown in Table 4.

We assume that the incident laser is a partially linearly polarizated beam with Stokes parameters $(I_i, Q_i, U_i, V_i) = (1, Q, U, 0)$. $I^{(t)}$, $I^{(d)}$ and η [Eqs. (11) and (12)] are simulated for fitting the measured η versus δ data, with $A_{\mathrm{pol}} = 4.327 \times 10^{-6}$ and $(Q, U) = (0, 0.22)$. The fitted η versus δ curve is also shown in

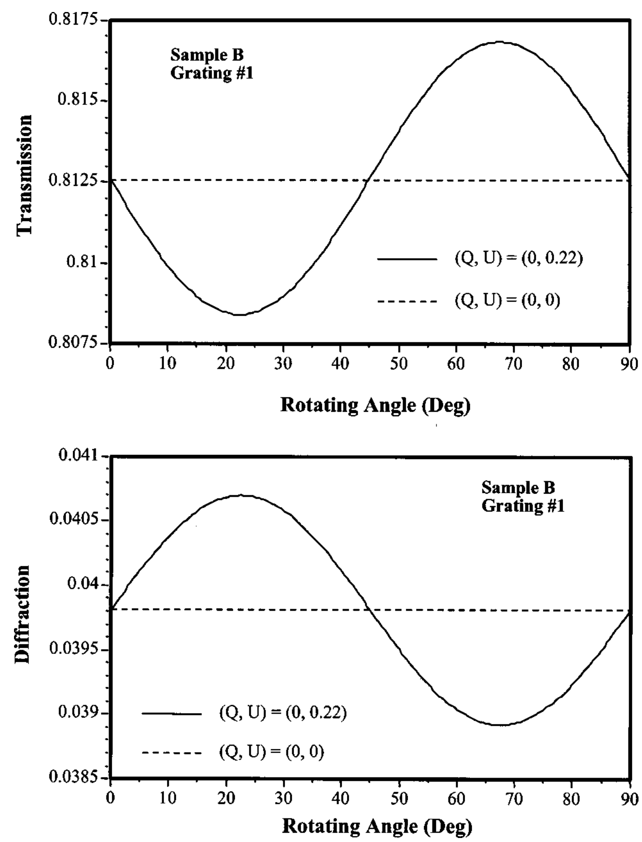

Fig. 9. HWP rotating angle (δ) dependence of the calculated transmittance of the transmitted and grating #1 diffracted beams at wavelength 532 nm. Parameters are the same as Fig. 8.

Fig. 7 (solid curve). Assuming $T_{\mathrm{hwp}} = 1$, the calculated transmittances $I^{(t)}$, $I^{(d)}$ versus δ curves are shown in Fig. 9. Similar fittings were done for the other two parameters $A_{\mathrm{pol}} = 3.439 \times 10^{-5}$ and 4.174×10^{-5}. The results are $(Q, U) = (0, -0.027)$ and $(0, 0.025)$, respectively. The fitted degrees of linear polarization are then determined to be 0.22, 0.027, and 0.025 for the three cases. The results show that the polarization-filtering power depends on the diffraction strength of the grating. The calculated Mueller matrix properties of the two beams (t and d) are listed in Table 4. The first-row Mueller matrix elements $M_{1k}^{(j)}$ ($j = t, d$; $k = 1, 2, 3, 4$) for signal calculation [Eq. (11b)] are shown.

6. DISCUSSION AND CONCLUSION

The measured Mueller matrices shown in Tables 2 and 3 demonstrate that there is nonvanishing depolarization ($\mathcal{D} > 0$). This depolarization is due to a statistical property that is neglected in the dynamic theory.[1,5,6] Therefore inclusion of depolarization is needed for a complete theory.

The measured and calculated polarization properties listed in Tables 2 and 3 show the birefringence. On the basis of Eq. (8), δn of the samples A and B are calculated; they are of the order of 10^{-4}. The results are listed in Tables 2 and 3. In addition, we measured that the substrate birefringence (reported in section 2) $\delta n = 3.42 \times 10^{-5}$. The substrate and grating birefringence of HBCS samples would be an interesting topic for further investigation.

As shown in Fig. 3, $A_{\mathrm{pol}}(\eta)$ is not a unique-valued function; it could not be determined by fitting the measured value of η only. As shown in Fig. 4 and Table 2, fitting the polarization parameters ψ and Δ is also an option. Therefore a scalar-field electromagnetic (EM) theory of strong coupling[10–14] could not completely determine the diffraction property (including polarization) of the VHG devices. Polarization characterization based on the vector field EM theory and the Mueller matrix[1] is necessary. Similarly, the η versus δ fitting curve in Fig. 7 is not unique. In addition to $(A_{\mathrm{pol}}, U) = (4.327 \times 10^{-6}, 0.22)$, we have other solutions, $(A_{\mathrm{pol}}, U) = (3.433 \times 10^{-5}, -0.027)$ or $(4.167 \times 10^{-4}, 0.025)$. The polarization parameters are listed in Table 4. All three cases give the same efficiency, $\eta = 0.0467$, in the absence of the rotating HWP. To get the diffraction-strength parameters A_{pol}, Cdn, $\Delta\delta_a$, and $\Delta\delta_b$, we fitted the ellipsometric parameters ψ and Δ, which were measured with high accuracy. The results are shown in Tables 2 and 3. Therefore a polarization measurement (ψ, Δ, or Mueller matrix) is needed for a full optical characterization of the holographic grating devices. The ellipsometric parameter Δ depends on the anisotropy modeling parameters Cdn, $\Delta\delta_a$, and $\Delta\delta_b$, whereas η and ψ depend only on the A_{pol} parameter. Although we have good fitting of Δ, the complicated $\Delta(A_{\mathrm{pol}})$ behavior shown in Fig. 4 has shown that it is an issue worth further investigation, both theoretically and experimentally. Our model is only the start of this investigation.

As shown in Table 1, the three gratings of sample B were designed to have the same incidence angle 2.17° for wavelength 532 nm. Assuming that the three gratings have approximately equal statistical weights, the transmittances of the transmitted (t) and the three diffracted ($d1, d2, d3$) beams and the total transmittance are calculated for $A_{\mathrm{pol}} = 0$ to 5×10^{-5}. The results, shown in Fig. 5, show that the intensity of each diffracted beam is ~1/3 of that of total diffraction. The incident beam is almost equally diffracted into three directions ($\Theta = 25.10°, 30.93°, 36.75°$). If operated in reverse, the three beams from different directions would combine to the same diffracted angle 2.17°. This is the principle of a holographic beam combiner.[8,9] Our theory[1] could be generally applied for simulating the performance of any HBCS device.

A HBS device can be applied to detect the polarization state of the incident radiation. An experiment and the fitted result were reported in Section 5. A three-hologram HBS device, specifically designed with the same incidence angle, can be applied to measure the Stokes parameters of incident light. The four measured signals of the transmitted (t) and the three diffracted ($d1, d2, d3$) beams are

$$S^{(j)}(\delta) = s_d I^{(j)}, \qquad j = t, d1, d2, d3, \tag{13a}$$

where

$$I^{(j)} = T_{\mathrm{hwp}}\{I_i M_{11}^{(j)} + Q_i M_{12}^{(j)} + U_i M_{13}^{(j)} + V_i M_{14}^{(j)}\}. \tag{13b}$$

A HBS-based Stokesmeter sensor can be developed on the basis of this principle. An engineering design of an optical system has recently been proposed for the electro-optics–infrared imaging-sensor application.[15]

In this paper we have concentrated only on the properties of single volume gratings. Properties of $N\langle\text{-}\rangle 1$ multihologram HBCSs would be worth further investigation. The birefringence and depolarization of the anisotropic substrate and sample with holographic gratings merits further study, as well. The application of the HBS for fabricating polarization-sensor optical devices is a challenging advanced electro-optics–infrared sensor technology.

The major conclusions are as follows:

1. Results of Mueller matrix measurement for holographic volume grating devices are reported we believe for the first time. The agreement with theoretical simulation is a justification of the theory.[1]
2. The vector EM theory is necessary for completely interpreting the diffraction property of a HBCS device.[1]
3. The theoretical and experimental foundation of HBS-based Stokes-meter optics for polarization-sensor technology is developed, we believe for the first time.

ACKNOWLEDGMENTS

This research was partially supported by the U.S. Office of Naval Research (ONR) through the NAVAIR/ONR ILIR Program, the NAVAIR Discretionary Fund, and the ONR Electro-Optics/Infrared Sensor Technology Program and by the MDA SBIR-II Program Contract N68936-01-C-0008.

T. W. Nee's e-mail address is tsuwei.nee@navy.mil.

REFERENCES

1. T. W. Nee and S. F. Nee, “Polarization of holographic grating diffraction. I. General theory,” J. Opt. Soc. Am. A **21**, 523–531 (2004).
2. S. F. Nee, “Measurement of reflective index of transparent materials using null polarimetry near Brewster angle,” in *Optical Diagnostic Methods for Inorganic Transmissive Materials*, R. V. Datla and L. M. Hanssen, eds., Proc. SPIE **3425**, 248–257 (1998).
3. S. F. Nee and H. E. Bennett, “Accurate null polarimetry for measuring the refractive index of transparent materials,” J. Opt. Soc. Am. A **10**, 2076–2083 (1993).
4. A. Knoesen and L.-M. Wu, “Absorption of polymers for optical waveguide applications measured by photothermal detection spectroscopy,” in *Linear and Nonlinear Optics of Organic Materials*, M. Eich and M. G. Kuzyk, eds., Proc. SPIE **4461**, 146–148 (2001).
5. S. F. Nee, “Polarization of specular reflection and near-specular scattering by a rough surface,” Appl. Opt. **35**, 3570–3582 (1996).
6. S. F. Nee, “Depolarization and principal Mueller matrix measured by null ellipsometry,” Appl. Opt. **40**, 4933–4939 (2001).
7. S. F. Nee, “Error analysis of null ellipsometry with depolarization,” Appl. Opt. **38**, 5388–5398 (1999).
8. M. S. Shahriar, J. Riccobono, and W. Weathers, “Holographic beam combiner,” in *Proceedings of the IEEE International Conference on Microwaves and Optics* (Institute of Electrical and Electronics Engineers, New York, 1999), pp. 10–14.
9. M. S. Shahriar, J. Riccobono, and W. Weathers, “Highly Bragg selective holographic laser beam combiner,” presented at the Solid State and Diode Laser Technology Review, Albuquerque, N.M., June 5–8, 2000.
10. H. Kogelnik, “Coupled wave theory for thick hologram gratings,” Bell Syst. Tech. J. **48**, 2909–2947 (1969).
11. C. B. Burckhardt, “Diffraction of a plane wave at a sinusoidally stratified dielectric grating,” J. Opt. Soc. Am. **56**, 1502–1509 (1966).
12. F. G. Kaspar, “Diffraction by thick, periodically stratified gratings with complex dielectric constant,” J. Opt. Soc. Am. **63**, 37–45 (1973).
13. S. Kessler and R. Kowarschik, “Diffraction efficiency of volume holograms,” Opt. Quantum Electron. **7**, 1–14 (1975).
14. R. Alferness, “Analysis of optical propagation in thick holographic gratings,” Appl. Phys. **7**, 29–33 (1975).
15. M. S. Shahriar, J. T. Shen, R. Tripathi, M. W. Kleinschmit, T. Nee, and S. F. Nee, “Ultrafast holographic Stokesmeter for active polarization imaging in real time,” Opt. Lett. **29**, 298–300 (2004).